PM vernier machine for utility scale wind generator applications: design and evaluation

---

Article:

Tlali, P.M., Wang, R-J. (2020) PM vernier machine for utility scale wind generator applications: design and evaluation, *Proc. of XXIV International Conference on Electrical Machines*, (ICEM), pp. 2637-2643, 23-26 August 2020, Gothenburg, Sweden (virtual conference)

ISBN: 978-1-7281-9944-3 / IEEE Catalogue Number: CFP2090B-USB

PM Vernier Machine for Utility Scale Wind Generator Applications: Design and Evaluation

P. M. Tlali, *Member, IEEE* and R-J. Wang, *Senior Member, IEEE*

***Abstract*—This paper investigates the feasibility of using permanent magnet vernier machine technology for large wind power applications. Optimal permanent magnet vernier machine designs rated at 1 MW and 3 MW and with different gear-ratios are generated through the use of multi-objective finite element based design optimization. The designs are then evaluated and also compared against the permanent magnet synchronous machine in terms of performance, costs, size and weight. Considering the power factor, the study shows that pole/slot combinations with gear ratios of 5 or less are more appealing since no substantial benefits can be claimed by going for higher gear ratio options. While the existing literature has mainly demonstrated its competitiveness relative to the permanent magnet synchronous machine for small machine sizes, it shows in this paper that the permanent magnet vernier machine also has a promising potential for being an alternative configuration in utility-scale wind-turbine drive-train applications.**

***Index Terms*—Design optimization, direct-drive generators, finite element analysis, magnetic gearing effect, permanent magnet vernier machines.**

I. Introduction

Wind power conversion has emerged as one of the most attractive and rapidly growing renewable energy resources. Research in this field has indicated a crucial need of developing innovative electrical machine technologies, as they are essential components in this application. Currently, a cascaded arrangement of mechanical gearbox and a medium- or high-speed machine is the common configuration implemented in wind turbine systems [1], [2]. However, to avoid gearbox issues and to improve on the system reliability, there has been a paradigm shift towards the use of direct-drive generators (DDGs) with full scale converters, especially in the offshore wind farms. Since the DDGs run at the low turbine speed, they usually have heavy structure and bulky sizes due to high torque handling requirements in utility scale wind energy conversion systems.

On the other hand, the past decade has seen a renewed interest in permanent magnet vernier machines (PMVM). As shown in Fig. 1, by putting the PMVM technology alongside current mainstream wind generator technologies, an interesting observation can be made, i.e. while the PMVM is more closely related to the direct-drive permanent magnet synchronous machine (PMSM), it also shares some characteristic properties with the medium-speed (MS) PMSMs due to its soft magnetic gearing features. This inherent magnetic gearing effect enables the PMVM to have high torque density, potential for lighter weight and more compactness than conventional PMSMs, while also maintaining the similar structural simplicity [3]–[5].

Despite the aforementioned advantages, the PMVMs are notably characterized by poor power factor that may increase the converter rating requirement and subsequently the system cost. Some studies have focused on the power factor improvement of PMVMs by proposing either more complex machine topologies (e.g. double-stator [6] or double-rotor [7]) or special permanent magnet (PM) arrangements (e.g. Halbach [8] or spoke-type [9]). Even though there are some comparison studies between PMVMs and conventional PMSMs in literature, these studies are limited to small power levels [10]. A quantitative analysis of the applicability and potential of PMVM technology for utility scale wind power applications is still lacking in the literature.

This paper aims at studying the feasibility of implementing the PMVM technology for large power wind generator systems. To achieve this goal, an finite element (FE) based design optimization study will be conducted for several selected PMVM topologies/design choices at 1 MW and 3 MW power levels. The realized designs will then be evaluated against a conventional PMSM of corresponding power rating.

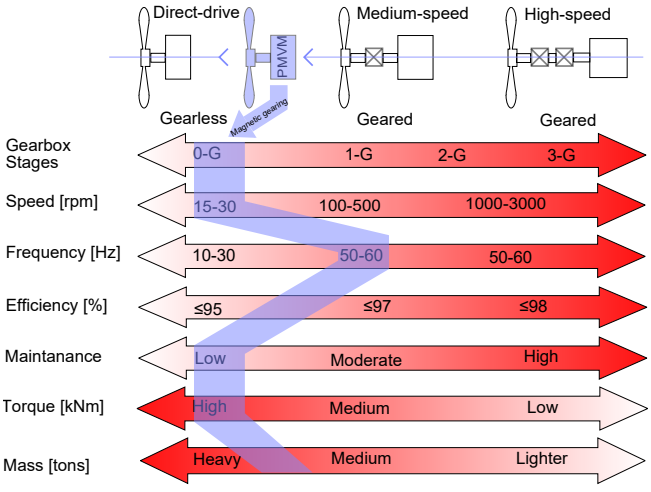

Fig. 1. PMVM vs. DD-PMSM and MS-PMSM characteristics at 3 MW power rating.

This work was supported by ABB Corporate Research, Sweden and the Consolidoc Award of Stellenbosch University in South Africa.

The authors are with the Department of Electrical and Electronic Engineering, Stellenbosch University, Stellenbosch 7600, South Africa (e-mail: 15894215@sun.ac.za; rwang@sun.ac.za)

The main objective in this case will be the reduction of total electromagnetic active material mass and cost while subjecting to the overall diameter constraint. That's because lighter and low cost machine is always a preferred choice in many applications including the wind energy conversion. The paper is organized as follows: Firstly, a brief description of the PMVM configuration will be provided in Section II, and this will be followed by the explanation of the implemented optimization strategy and specifications in Section III. Then the obtained results are presented and discussed on Section IV, after which a conclusion will be drawn in Section V.

II. Basic PMVM Configurations

PM vernier machines operate on the same magnetic gearing principle as in coaxial flux modulated magnetic gears (CMGs). That is, a high-speed low-order space harmonic field is generated by the stator windings, whereas the low-speed high-order space harmonic field originates from the rotor PMs. The two field harmonics are magnetically coupled through modulation by the ferro-magnetic pole-pieces (flux modulator), which is situated in-between their respective exciting components. Flux modulator can be in the form of a separate component, or a split stator teeth or even the stator teeth themselves. For the magnetic gearing principle to be effectively realized in PMVMs, the numbers of winding pole-pairs (p_s), rotor pole-pairs (p_r) and flux-modulator pole-pieces (N_s) are strictly related by [11], [12]:

$$N_s = p_r \pm p_s \tag{1}$$

The number of stator teeth/slots (Q_s) can then be separately selected according to the applicable rules to achieve stable field generation with balanced phase flux linkages at chosen frequency. However, in the case of the PMVM type where the stator teeth also perform the modulation function (Fig. 2a), it means the stator-slots number is the same as that of the modulating pieces, hence N_s can be replaced by Q_s in (1). The cross-sectional views of some of the typical structure configurations of PMVMs are presented in Fig. 2.

Skaar and Nilssen provided a fairly clear approach to calculating the winding factors of the tooth concentrated

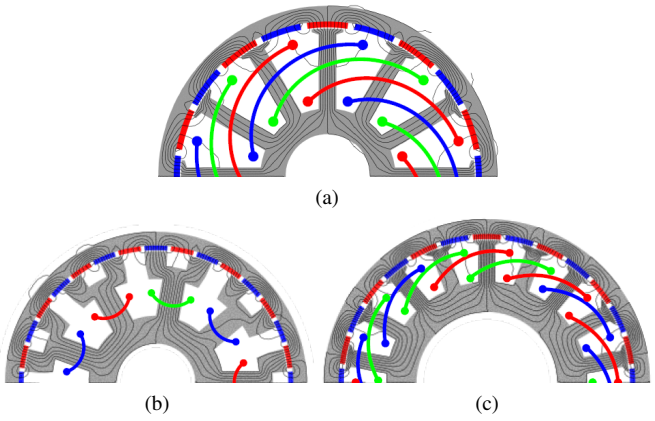

Fig. 2. Typical structures of PMVM machines: (a) Conventional overlap-winding (b) Tooth concentrated, split tooth (c) Two-slot pitch winding.

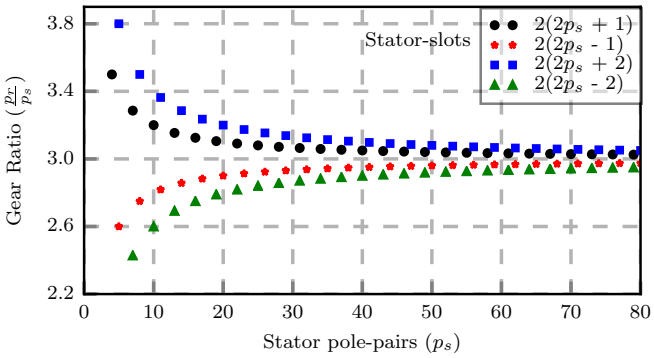

Fig. 3. Gear ratios of two-slot pitch PMV machines.

one-slot pitch winding PMSMs, and concluded that based on the value of the number of slots per-pole per-phase q, a feasible region of reasonable winding factors would be $\left(\frac{1}{4} < q < \frac{1}{2}\right)$ [13]. Furthermore, the same study showed that all other pole/slot combinations have a balanced air-gap magnetic radial forces except those with Q_s=$2p_s \pm 1$. To reduce the unbalanced force magnitudes in pole/slot combinations utilizing this winding arrangement, one technique is to double the number of slots while the pole number remains the same. Based on this observation, the two-slot pitch windings were developed (Fig. 2c), and their implementation on PMVMs was demonstrated by several researchers [14]. For the PMVM development, this type of winding is obtained by just doubling the number of slots from the one slot-pitch winding conventional PM machines, including those with balanced magnetic forces. In this case, the purpose of doubling the slot number with no change in original armature poles is to create a bigger numerical difference between them, and this gives more design flexibility which can easily satisfy (1). This then results in a new range of q values with no negative impact on winding factor, i.e. $\left(\frac{1}{2} < q < 1\right)$, and other advantages from their original one slot-pitch are retained. Most of the single slot-pitch combinations always gives acceptable two-slot pitch windings except those with the basic ratio $\frac{Q_s}{2p_s}$=$\frac{3}{2}$. Considering all the applicable conditions in developing this type of winding, the gear ratios of PMVM utilizing it are defined by (2). It can be clearly seen that the G_r is confined within a range of $(2 < G_r < 5)$, and converges to 3 as the stator winding pole-pair number is increased, shown in Fig. 3.

$$G_r = 3 \pm \frac{2}{p_s} \quad \text{and} \quad G_r = 3 \pm \frac{4}{p_s} \quad \text{with} \quad p_s > 2 \tag{2}$$

III. Design Optimization Process

For the design and performance evaluation of PMVMs, the corresponding specifications and parameters range of PMSMs, such as input speed, operating frequency, total outer diameter and stack length, etc., are used as a benchmark and reference guide. So, a highlight on PMSMs' performance and characteristic properties is first given as a preset to the

PMVM's specifications. In addition, the design constraints, procedure and strategy are also described in this section.

A. Specifications

Since the optimization objectives are primarily concerned with the active material weight and volume, a presentation of these characteristic parameters for a PMSM is given in Fig. 4 as obtained from the literature. This is done for a 1 MW, 3 MW and 5 MW machine output levels to indicate their characteristic relationship against rating up-scaling as well. As these machines were optimized by different researchers based on various specifications, constraints and algorithms, there is a bit of variance in their performance at each rated level. Hence the ranges in the figure indicate the dispersion of active weight and volume highlighting the minimum and maximum values as obtained from the relevant literature. By considering their averages, both the active material weight and volume shows somewhat linear trend against the machine power rating. Furthermore, it appears from Fig. 4 that about 16.5 tons mass and 20 m^3 volume are deemed reasonable for a 3 MW DD-PMSM generator.

A break down of different material types contributing to the machines' active weights provided in Fig. 4 is also shown by Fig. 5. As seen in the figure, the lamination mass is always the most dominant since it takes at least 60 % of the total mass. On the other hand, the PM material contributes the least percentage mainly because of its smaller volume requirement relative to other material types and also because of its slightly lower mass density. Therefore, Fig. 5 shows that the lamination material is the main deciding factor on the PMSM machine's total electromagnetic active weight.

Based on the above information, the main design specifications are provided on Table I. A minimum efficiency of 94 % is specified for 300 kW machines or less, while 95 % is required for 1 MW machines and above. As the output capacity of the machine is increased to the mega-Watt level, the available wind speed distribution, generator physical size and that of turbine blades dictates the rated speed be decreased accordingly and the frequency should follow similar trend to limit the core-losses. Theoretically, larger air-gap radius would also be needed to accommodate high number of poles and handle large input torque from the blades. But factors

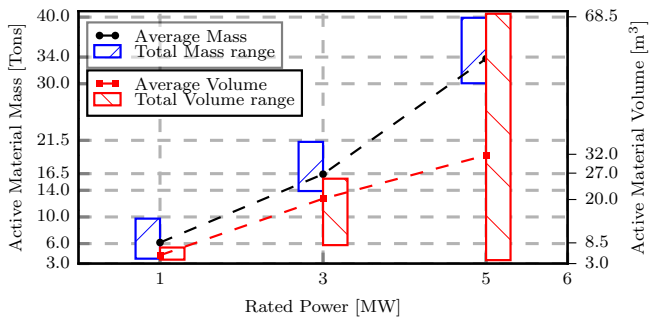

Fig. 4. Active mass and volume of PMSM as function of power rating found from the literature.

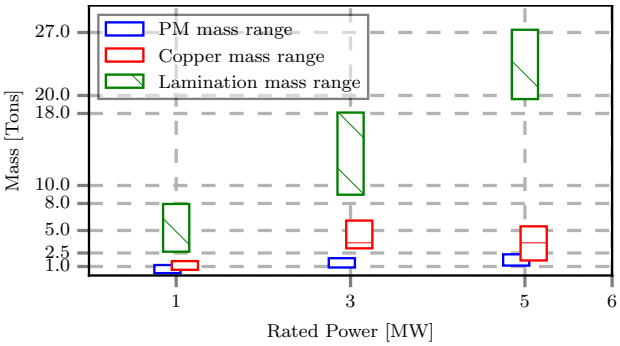

Fig. 5. Different active material weight distribution vs. power rating of PMSM.

such as available nacelle size, manufacturing and logistic constraints put the upper limits as to how large a machine can be. So, the total outer diameter (D_{out}) of active volume is considered in this case to give an approximate size of machine, and the air-gap radius will be determined by the optimization variables. It is assumed that no special cooling methods will be implemented for the machines, hence an armature current density of 5 A/mm^2 is set to be the upper limit as for a natural air-cooled machine. Considering the strong magnetic attraction forces and manufacturability of the machine, a reasonable air-gap length corresponding with machine size should be selected, which is taken to be roughly 0.1 % of the total diameter in this study.

TABLE I
MAIN DESIGN SPECIFICATIONS OF MACHINES AT DIFFERENT POWER LEVELS [1], [15]–[21].

Parameter	60 kW	300 kW	1 MW	3 MW
Maximum diameter (m)	1.2	2.5	3.5	5.0
Air-gap length (mm)	3.0	4.0	4.0	5.0
Rated speed (rpm)	80	50	30	20
Efficiency (%)	≥94	≥95	≥95	≥95
Current density (A/mm^2)	≤5	≤5	≤5	≤5

B. Methodology

A hybrid optimization approach was implemented, whereby a stochastic and a gradient based algorithms, i.e. Non-dominated Sorting Genetic Algorithm II (NSGA-II) and Method of Modified Feasible Directions (MMFD) respectively, were used in two sequential steps to obtain one best final solution. The NSGA-II is initially used to determine the search region that contains the global optimum within it. Once in this general vicinity of the global optimum, the MMFD is used with the NSGA-II's results as the starting point to quickly locate the precise optimum point by further zooming into the solution area. In this way, the two algorithms are combined and efficiently employed to find a true optimum point within much reasonable time. That is because, since the MMFD started from an already improved point, it will quickly converge with less number of evaluation iterations than what would be required if NSGA-II would be

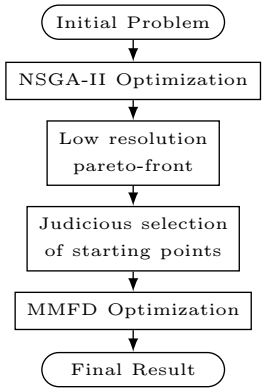

Fig. 6. Hybrid optimization technique work flow.

used alone to find the very best point. Fig. 6 illustrates the work-flow of this optimization technique.

In NSGA-II, a number of user-adjustable operators has to be fine tuned based on the characteristics of the optimization problem in order to enhance the algorithm's efficiency and reliability. The settings of these specific parameters are given in Table II for the optimization of all machines (1 MW and 3 MW). A fixed initial population size of 60 was also used for all optimization trials, which is five-times the number of optimizations variables and deemed reasonable according to NSGA-II theory as a lager populations size would drastically increase the number of solver evaluations and optimization time. The maximum number of generations was set to 600 for 1 MW machines and increased to 1200 for 3 MW machines because the purpose of the NSGA-II in this case was just to identify the zone of global optimum but not to arrive at an absolute optimum point which would definitely need a much larger value. The mutation probability was set to 0.0833, which is the reciprocal of the variables number (i.e. 12) as per the relevant theory of NSGA-II as well [22].

The formulated optimization problem has more than one objectives and several design constraints as follows:

$$\begin{aligned} \text{Minimize:} \quad & F(\mathbf{X}) = [\mathbf{Y}] \\ \text{Subject to:} \quad & P_{\text{out}} \geq \text{P}_{\text{rated}} \\ & \eta\,\% \geq \eta_{\text{min}} \\ & J \leq 5\,\text{A/mm}^2 \end{aligned}$$

where $\mathbf{X}$ represents the vector of geometric variables illustrated in Fig. 7 with angle ratios defined in (3), including the axial stack length of the machine, and $\mathbf{Y}$ is one or a set of selected objective functions. That is, the objectives

TABLE II
NSGA-II USER ADJUSTABLE PARAMETERS' SET VALUES.

Parameter	Value
Initial population size	60
Maximum iterations	600 - 1200
Probability of mutation	0.08333
Disindex of mutation	12
Probability of cross-over	0.99
Disindex of cross-over	16

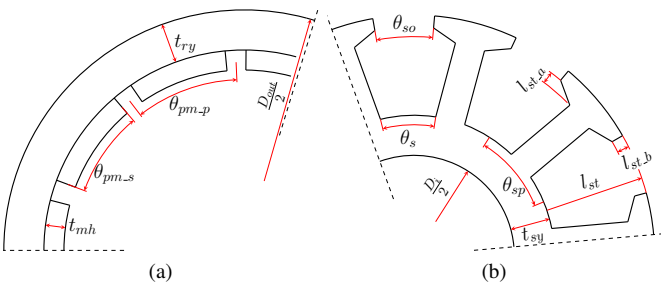

Fig. 7. Machine geometric optimization variables: (a) Rotor (b) Stator.

include minimization of mass and cost. The minimum powers and efficiencies are as indicated in Table I for each power rating. It should also be noted that the temperature and material characteristics were kept constant throughout the optimization process.

$$\begin{aligned} \theta_{pm\_p} = \frac{\pi}{p_r} \quad ; \quad \theta_{sp} = \frac{2\pi}{Q} \quad ; \quad \theta_{mp} = \frac{2\pi}{N_s} \\ \sigma_{pm} = \frac{\theta_{pm\_s}}{\theta_{pm\_p}} \quad ; \quad \sigma_s = \frac{\theta_s}{\theta_{sp}} \quad ; \quad \sigma_{so} = \frac{\theta_{so}}{\theta_s} \end{aligned} \tag{3}$$

IV. Optimization Results and Discussions

As a preliminary design exercise, the PMVMs are designed and optimized for a rated power of 1 MW. A comparison is made of the power factor and the active weights at a number of different gear ratios. This is to investigate the relations between the gear ratios and the design objectives of large power PMVMs. As shown in Fig. 8, in distributed overlap winding (OW) machines with ($G_r \geq 5$), lower gear ratio designs are preferred as they tend to have higher power factor and lighter mass. Further, these Pareto fronts clearly reveal the competing relationship between the active mass and power factor in PMVMs.

Fig. 9 shows the optimum designs of PMVMs with both distributed OW ($G_r \geq 5$) and 2-slot pitch concentrated winding (CW) ($G_r \leq 5$) configurations. The graphs illustrate the trend of active mass and power factor as a function of gear ratios at two different frequencies. It can be clearly seen that the mass increases with the gear ratio while the power factor decreases. It should be remembered that the minimum constraint on power factor was set to 0.65 during the optimization, and higher gear ratio designs appear to be testing this threshold, giving an impression that it would likely go lower than that if the constraint was relaxed. It is at this rated power level that the two-slot concentrated winding (CW) machines ($G_r \leq 5$) appear to be more attractive in terms of power factor and light weight than the conventional distributed OW machines.

As a benchmark, the average DD PMSM weight is also added on Fig. 9 for comparison. Although not shown on the graph, PMSM is known to have a near unity power factor. Thus, all the PMVM designs here have poor power factor comparing with the PMSM. But the distributed OW PMVMs with gear ratio of 5 and the 2-slot-pitch CW PMVMs are

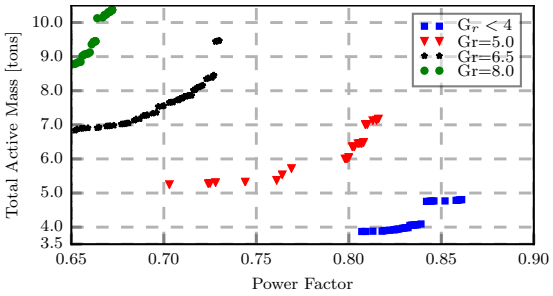

(a)

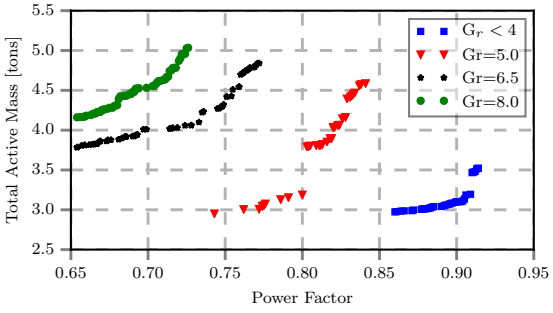

(b)

Fig. 8. 1 MW machine's active mass vs. power factor: (a) 30 Hz (b) 60 Hz.

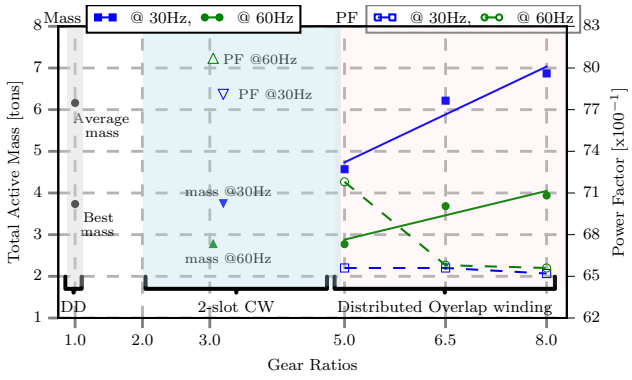

Fig. 9. Total active mass versus gear ratios for 1 MW machines.

much lighter than the DD PMSM. There is clearly a tradeoff between the light weight and poor power factor in PMVMs.

It can be observed from the results of 1 MW machines that PMVM designs with operating frequency similar to that of their conventional DD-PMSM counterparts offer no significant benefits. Therefore, for the 3 MW design, the decision was made to go for slot/pole combinations that operate at medium-speed frequency ($\approx$ 50 Hz) but with equivalent turbine input speed to the DD-PMSMs, since their core-losses are not so different. That is, in addition to the gearing ratio, the generators' rated speed and output frequency were also the main factors considered in selection of the slot/pole combinations as presented in Table III.

For the PMV machine, the power factor is one of the performance indexes that always need a special attention as it can come out to be detrimental if not properly designed. With that said, Fig. 10 shows the Pareto-front between the total active mass and power factor for the five 3 MW PMV

TABLE III
INVESTIGATED SLOT/POLE COMBINATIONS FOR 3 MW PMV MACHINES.

Winding configuration	**2-slot CW**		**Distributed OW**		
Stator slots (Q_s)	270	276	240	240	225
Stator pole-pairs (p_s)	67	68	40	32	25
Rotor pole-pairs (p_r)	203	208	200	206	200
Pole-ratio (G_r)	3.03	3.06	5.00	6.50	8.00
Slots per pole per phase (q)	0.67	0.68	1.00	1.25	1.50
Rated frequency [Hz]	50.75	52.00	50.00	52.00	50.00

machine slot/pole combinations and having different gear ratios. During the optimizations, the upper limit to the PM material usage was set to be equal to the maximum PM mass requirement of the reference PMSGs indicated in Fig. 5, and the minimum efficiency was set to be 95 %. Since the PMV machines have similar input speeds to those of the PMSGs, this means a fairly similar ground is created for the comparison purposes in these two machine types to be presented later in this section. From the figure, the higher gear ratios seemingly lead to lower power factors and heavier total masses. Furthermore, it is realized that some of the PMV slot/pole combinations can lead to poor power factors with values less than 0.4. This further asserts the point that at output power capacities larger than 1 MW, it is always better to go for lower gear ratio if any benefits are to be obtained from this type of machine.

In order to estimate the cost of the active materials in a machine, the specific cost of each material has to be known. Table IV contains the material prices used in this study, which may be slightly different to the market values. Based on the literature [1] and the market trend, 35 $/kVA was assumed to be the cost for the converter. It should be noted that in industry the actual converter prices usually follow a stepped profile instead of this kind of linearized costing model.

TABLE IV
APPROXIMATE COSTS OF DIFFERENT MATERIALS FOR PMSM COMPONENTS [23].

Material	**Cost per kilogram ($/kg)**
Silicon steel (Lamination)	2.0
Copper (Winding)	6.67
Neodymium Iron Boron (PM)	50.0

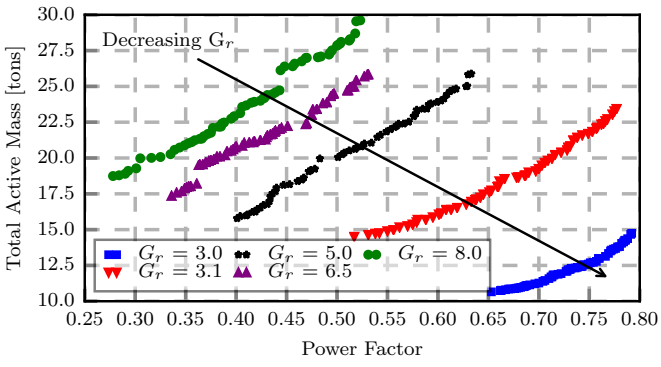

Fig. 10. Total active mass vs. power factor for 3MW PMV machines.

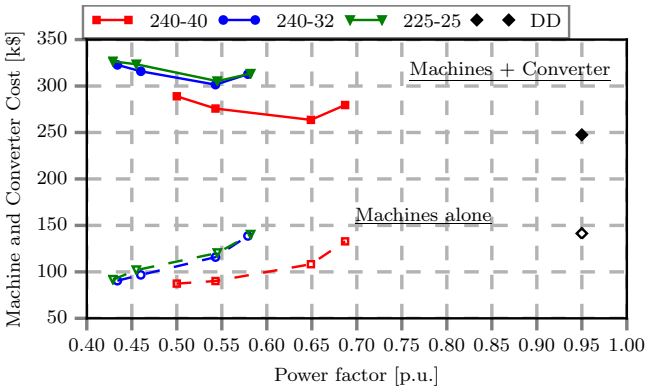

(a)

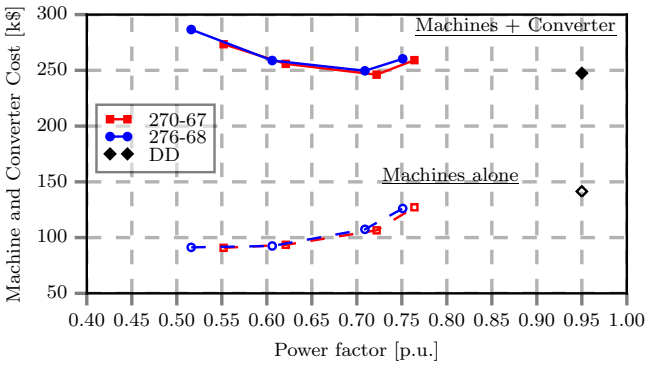

(b)

Fig. 11. Comparison of machine and total system costs: (a) Distributed overlap-winding PMVM (b) Two-slot CW PMVM.

In order to compare the PMV machines with the PMSM, one design point for each slot/pole combination was taken from the Pareto-fronts given in Fig. 10 and further optimized. The objective in this case was to have a lighter and cheaper PMV machine with best possible power factor. The results are presented in Figs. 11a and 11b, and on Table V, with the indicative costs of materials also included.

Even though Silicon steel used for machine cores has slightly lower mass density than winding copper, it has the largest impact on the total active mass because of its larger volume content. The machines' efficiencies are always higher than minimum constraint of 95 % even though the operating frequency is relatively high. Increasing the PM mass has relatively little effect on total active mass, but it can significantly increase the cost of the machine and slightly improve the power factor. Figs. 11a and 11b show that a cheaper machine with low power factor leads to an expensive system when the power converter costs are included. Thus, to select a good design, a best compromise has to be found between the machine cost and required converter cost.

Fig. 12 shows the mass distribution of the chosen designs and compares them to the benchmark PMSG. PMV machines with lower gear ratios have a good advantage in terms of total active weight. In summary, designing for a lighter machine with reasonable power factor at this power rating, requires choosing a pole/slot combination with lower G_r. This is a

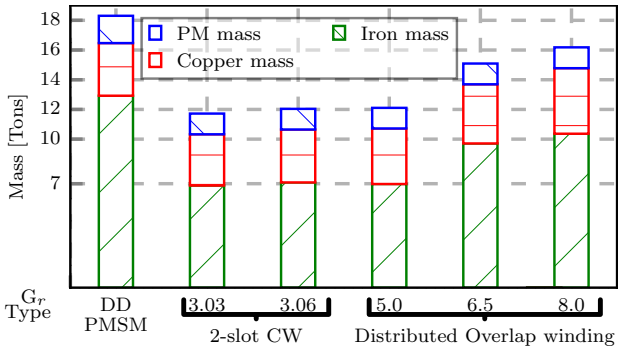

Fig. 12. Comparison of active material weights of PMSM and PMVMs.

somewhat different trend to the small power PMVMs where the lowest G_r values are not necessarily the best.

The results in Table V reveal that the PMVM on its own can be lighter and cheaper than the PMSM. But when the power converter costs are considered, the overall system costs of PMVMs become similar to those of DD PMSMs because of their high converter rating requirement. It should be noted that a linear inverter costing model was assumed in this study, which may not necessarily reflect the true costs in industry. In the case that the inverter costs follow a stepped increasing pattern with regard to their MVA rating, the cost of PMV generator systems may become competitive for certain power levels. Furthermore, the PMV machines' power factor gets improved if the total volume is allowed to increase with longer stack lengths, but this will inevitably lead to large size machines, which are unfavorable.

V. Conclusions

This paper presents an investigation study on the potential design of PMVM for large power wind generator applications. It is observed that, lower gear-ratios are more attractive to achieve optimum machines with reasonable total mass and power factor at utility scale power levels, while this is not so apparent in small power machines. The lower PM material usage in a PMVM machine is advantageous as this translates to a low cost design (about 20 % cheaper than an equivalent PMSM machine at 3 MW level), but this advantage is offset by the cost of bigger converter capacity needed for a PMVM, which at the end brings the total cost of the two systems to level up. Even though the PMVM is designed to operate at a direct-drive generator input speeds, its operating frequency may need to be in the same range as that of medium-speed generators in order to enhance its best potential. This implies that its inherent soft gearing effects makes it an intermediate alternative between the direct drive and medium-speed concepts. The study predicts that it is feasible and economically reasonable to develop a MW output level PMV generator for the wind power applications.

References

[1] H. Polinder et al., "Comparison of direct-drive and geared generator concepts for wind turbines," *IEEE T-EC*, 21(3):725-733, Sep. 2006.

TABLE V
MASS AND COST COMPARISONS OF DIFFERENT 3 MW PMSG ([15], [19]) AND PMV MACHINES.

Machine type	**DD PMSG**		**2-Slot CW PMV**		**Distributed OW PMV**		
Rotor/Stator pole-ratio	1.0	1.0	3.0	3.05	5.0	6.5	8.0
Characteristic Information							
Output power (MW)	3.00	3.00	3.04	3.06	3.00	3.04	3.04
Efficiency (%)	95.0	-	95.91	95.93	97.06	97.08	97.77
Power factor	0.93	-	0.72	0.71	0.65	0.54	0.55
Average torque (kNm)	1910.0	-	2006.8	2020.5	1943.5	1981.5	1962.7
Total diameter (m)	5.000	5.00	5.000	5.000	5.000	5.000	5.000
Stack length (m)	1.300	1.190	1.403	1.399	1.378	1.377	1.372
Material Mass contributions (tons)							
Rotor PM	1.90	1.92	1.39	1.39	1.39	1.40	1.40
Core iron	10.30	11.70	6.87	7.08	6.98	9.71	10.36
Winding copper	3.12	3.31	3.45	3.56	3.74	3.98	4.41
Total generator mass	13.38	16.90	11.72	12.04	12.11	15.09	16.18
Machine cost distributions (k$)							
Rotor PM	95.00	96.00	69.50	69.50	69.50	70.00	70.00
Core iron	20.60	23.40	13.74	14.16	13.96	19.42	20.72
Winding copper	20.81	22.08	23.01	23.75	24.95	26.55	29.41
Total generator	**136.41**	**141.48**	**106.25**	**107.41**	**108.41**	**115.97**	**120.13**
PE converter	108.39	106.11	140.0	142.0	155.1	186.7	183.3
Total system	244.8	247.59	246.25	249.41	263.51	388.9	303.43

[2] R.-J. Wang, S. Gerber, "Magnetically geared wind generator technologies: Opportunities and challenges," *Applied Energy*, 136:817-826, 2014.

[3] S. Gerber, R.-J. Wang, "Design and evaluation of a PM vernier machine," in *IEEE Energy Conversion Congress and Exposition (ECCE)*, Sept 2015, pp. 5188–5194.

[4] J. Li et al., "A new efficient permanent-magnet vernier machine for wind power generation," *IEEE T-MAG*, 46(6):1475-1478, June 2010.

[5] G. Liu et al., "A new modeling approach for permanent magnet vernier machine with modulation effect consideration," *IEEE T-MAG*, 53(1):1-12, Jan 2017.

[6] C. Liu, K. T. Chau, Z. Zhang, "Novel design of double-stator single-rotor magnetic-geared machines," *IEEE T-MAG*, 48(11):4180-4183, Nov 2012.

[7] S. Niu et al., "Quantitative comparison of novel vernier permanent magnet machines," *IEEE T-MAG*, 46(6):2032-2035, June 2010.

[8] D. Li, R. Qu, Z. Zhu, "Comparison of halbach and dual-side vernier permanent magnet machines," *IEEE T-MAG*, 50(2):801-804, Feb 2014.

[9] W. Liu, T. A. Lipo, "Analysis of consequent pole spoke type vernier permanent magnet machine with alternating flux barrier design," *IEEE T-IA*, 54(6):5918-5929, Nov 2018.

[10] P. M. Tlali, R.-J. Wang, S. Gerber, C. D. Botha, M. J. Kamper, "Design and performance comparison of vernier and conventional PM synchronous wind generators," *IEEE T-IA*, 56(3):2570-2579, May/June 2020.

[11] B. Kim, T. A. Lipo, "Design of a surface PM vernier motor for a practical variable speed application," in *2015 IEEE Energy Conversion Congress and Exposition (ECCE)*, Sept 2015, pp. 776–783.

[12] ——, "Operation and design principles of a PM vernier motor," *IEEE T-IA*, 50(6):3656-3663, Nov 2014.

[13] S. E. Skaar, Ø. Krøvel, R. Nilssen, "Distribution, coil-span and winding factors for PM machines with concentrated windings," in *Int'l Conf. on Electrical Machines (ICEM)*, Sept. 2006.

[14] K. Wang, Z. Q. Zhu, G. Ombach, "Synthesis of high performance fractional-slot permanent-magnet machines with coil-pitch of two slot-pitches," *IEEE T-EC*, 29(3):758–770, Sept. 2014.

[15] J. H. J. Potgieter, M. J. Kamper, "Double PM-Rotor, toothed, toroidal-winding wind generator: A comparison with conventional winding direct-drive PM wind generators over a wide power range," *IEEE T-IA*, 52(4):2881–2891, July 2016.

[16] D. Ban et al., "Generator technology for wind turbines, trends in application and production in Croatia", Engineering, Environmental Science, 2007.

[17] A. Grauers, "Design of direct driven permanent magnet generators for wind turbines," Ph.D. dissertation, School of Electrical and Computer Engineering, Chalmers University of Technology, 1996.

[18] T. D. Strous, U. Shipurkar, H. Polinder, J. Ferreira, "Comparing the brushless DFIM to other generator systems for wind turbine drive-trains," *Journal of Physics: Conference Series*, vol. 753, 05 2019.

[19] H. Li, Z. Chen, H. Polinder, "Optimization of multibrid permanent-magnet wind generator systems," *IEEE T-EC*, 24(1):82-92, March 2009.

[20] X. Yang, D. Patterson, J. Hudgins, "Permanent magnet generator design and control for large wind turbines," in *IEEE Power Electronics & Machines in Wind Applications*, July 2012, pp. 1–5.

[21] W.-C. Tsai, "Robust design of a 5MW permanent magnet synchronous generator using Taguchi method," in *2012 7th Int'l Conf. on Computing & Convergence Technology (ICCCT)*, Dec 2012, pp. 1328–1334.

[22] K. Deb, A. Pratap, S. Agarwal, T. Meyarivan, "A fast and elitist multiobjective genetic algorithm: NSGA-II," *IEEE Trans. Evolutionary Computation*, 6(2):182-197, April 2002.

[23] M. Johnson et al., "Design, construction, and analysis of a large-scale inner stator radial flux magnetically geared generator for wave energy conversion," *IEEE T-IA*, 54(4):3305-3314, July 2018.

Pushman M. Tlali is a native of Leribe, Lesotho. He obtained his B.Eng in Electrical and Electronic Engineering in 2012, and further received his M.Eng and the Ph.D. degrees in electrical engineering from Stellenbosch University, South Africa in 2015 and 2019, respectively. He is currently a postdoctoral research fellow at the same university in the field of electrical machines, with a specific focus on magnetically geared PM machines. His research interests are in the design and optimization of rotating electrical machines, and renewable energy power generation.

Rong-Jie Wang received the M.Sc. degree in electrical engineering from University of Cape Town in 1998 and the Ph.D. degree in electrical engineering from Stellenbosch University in 2003, all of South Africa. He is currently an Associate Professor with the Department of Electrical and Electronic Engineering at Stellenbosch university. His research interests include novel topologies of permanent magnet machines, computer-aided design and optimization of electrical machines, cooling design and analysis, and renewable energy systems. Dr. Wang is a co-author of the monograph *Axial Flux Permanent Magnet Brushless Machines* (Springer 2008)